Scattering of He atoms from KCN(001): Analysis of the energy exchange

Srilal M. Weera and J. R. Manson
Department of Physics and Astronomy, Clemson University, Clemson, South Carolina 29634

Jeff Baker, E. S. Gillman, J. J. Hernández, G. G. Bishop, S. A. Safron, and J. G. Skofronick
Departments of Physics and Chemistry and Center for Materials Research and Technology, Florida State University, Tallahassee, Florida 32306

(Received 1 May 1995; revised manuscript received 10 July 1995)

High-resolution inelastic He-atom surface scattering experiments have been carried out on an *in situ* cleaved KCN(001) molecular crystal surface in the temperature range of $40 < T < 334$ K covering the temperature range of the two known bulk phase transitions at 168 and 83 K. No Bragg diffraction peaks other than the specular beam are observed over the entire temperature range. The scattering intensity is primarily composed of inelastic multiphonon processes along with some diffuse elastic-scattering contributions, the latter of which increases in magnitude with decreasing temperature while the former decreases in intensity with decreasing temperature. A theoretical model developed for explaining the multiphonon-scattering process gives very good quantitative agreement with the data.

I. INTRODUCTION

The inelastic scattering of nearly monoenergetic helium atoms from crystal surfaces in single-phonon collisional experiments has provided important information about fundamental dynamical processes occurring at surfaces.[1] More recently, experiments have been carried out which focus on the multiphonon contribution to the scattering process.[2–7] Normally, this component is observed as a broad inelastic background upon which the elastic and single-phonon peaks often appear. Although it resembles a diffuse background, it is nonetheless still coherent, and under many circumstances can exhibit distinctive features such as broad peaks or valleys. A quantum-mechanical theory has been developed[8,9] which is capable of analyzing the multiphonon scattering of particles with small mass, such as He, under the conditions of the experiment reported herein. An approximate semiclassical limit has also been derived which is valid for conditions where the Debye-Waller exponent $2W$ is large, namely $2W > 6$, which occurs under conditions that combine high surface temperatures, high-energy particles and large mass projectiles. Much of the previous work, both experimental and theoretical, has concentrated on close-packed metal surfaces such as Cu(001) and on insulator surfaces such as the alkali halides LiF, NaCl, RbCl, and KBr.[2–9] This work now extends the measurements and analysis to a molecular crystal KCN(001) which has vibrational properties similar to the alkali halides, and in addition exhibits molecular motion of the CN^- ion.

KCN belongs to a broad group of polymorphic compounds which have the form $M^+(XY)^-$, where M^+ is a positive metal ion and XY^- is a linear molecular negative ion. Immediately below the melting point they typically exhibit cubic structure, and may undergo one or more structural phase transitions as the temperature is lowered.[10] KCN is known to have three phases in the bulk with the two phase transitions occurring at 168 and 83 K. In the high-temperature phase ($T > 168$ K), KCN is a transparent crystal with a NaCl-type structure that has CN^- ions in an octahedral cage comprised of six K^+ ions. There is no orientational order of the CN^- ions with respect to the octahedral cage. At $T = 168$ K, KCN transforms to a body-centered-orthorhombic structure with the CN^- ions orienting along the "b" direction which corresponds to the $\langle 110 \rangle$ axes of the cubic rock-salt phase.[11] This structure remains until $T = 83$ K, where KCN transforms to a monoclinic phase in which the CN^- ions align alternately in the $\langle 110 \rangle$ direction and, consequently, the crystal becomes antiferroelectric.[10–12]

Neutron inelastic scattering and Raman measurements made on bulk KCN implicate multiphonon effects in such features as the high degree of dynamic disorder of the CN^- ion and the unusually large Debye-Waller exponents which were observed.[10,12–15] These features are also found in the He-atom surface scattering studies reported in this paper. Since the cleaving of a KCN crystal removes one of the six K^+ ions which cage the CN^-, one expects that even greater dynamic disorder should be present for the surface studies. The KCN surface is thus expected to behave similarly to a crystal surface with loosely bound molecular adsorbates which can exhibit hindered translational and rotational motion.

II. EXPERIMENT

The apparatus employed for the experimental work is described briefly below. Details are given elsewhere.[16] Its design is similar to other He-atom scattering (HAS) instruments described in the literature.[17,18] The geometry of the system is fixed such that the helium atoms which scatter from the target have the sum of their incident and final scattering angles measured with respect to the surface normal equal to 90° ($\theta_i + \theta_f = 90°$). There

0163-1829/95/52(19)/14185(7)/$06.00

are two modes of operation of the instrument: (1) with the chopper out of the beam path, and (2) with the chopper in the beam path. For the former, there is no energy analysis of the scattered beam, and the measurements consist of the scattering intensity versus incident angle, called an angular distribution. Usually such measurements contain specular and Bragg scattering peaks which give general structural information about the surface. In the second or time-of-flight (TOF) mode of operation, the measurements are done at fixed incident beam energy and fixed incident and scattered angles θ_i and θ_f. The chopper produces 7-μs pulses from the beam and the energy-transfer information is obtained from the resulting TOF spectra.

The two different KCN crystals used in this work were approximately $6\times7\times2$ mm^3 in dimension, cut from a boule obtained from the University of Utah Crystal Growth Lab.[19] Both targets were produced by cleaving *in situ* to yield the (001) surface. For the first target the chamber pressure was in the low 10^{-10}-torr range, and for the second in the mid-10^{-11}-torr range. Each of the samples was mounted on an oxygen free high conductivity (OFHC) sample holder attached to the manipulator. Prior to the cleave, the target chamber was baked to 150 °C for about 15 h. Two types of cleaves were employed. For the first target the cleave was made by using the closing of two jaws on a notched crystal, while for the second the cleave was obtained from a spring-driven guillotine device.

After producing the targets, angular distributions were taken at temperatures which ranged across all three phases of bulk KCN. Despite considerable effort and care in searching, no Bragg peaks were observable over the crystal temperature range from 35 to 300 K, thus indicating the absence of long-range order at the surface of the crystal. Hence it was not possible to align the target in the $\langle 100\rangle$ or $\langle 110\rangle$ high-symmetry directions from the diffraction pattern, as is normally done with the alkali halides. Rather the alignment in these directions was done based on the geometry of the crystal and its cleavage planes and the approximate cosine shape of the measured angular distributions. A series of TOF spectra were taken as a function of temperature from 35 to 300 K in each of the two high-symmetry directions, mostly at the approximate specular angle but also with a few spectra taken in nonspecular directions. The second crystal gave similar results to the first, but was superior in quality, and thus the results for it are the ones reported in this paper.

The incident He beam energy in this instrument can be varied from about 20 to 60 meV, with an energy width of about 2% full width at half maximum (FWHM) by controlling the temperature and the pressure of the nozzle beam source. For the measurements reported here the energies were near 30 meV, corresponding to incident wave vectors of ≈ 7.6 Å^{-1}.

III. THEORY

The quantum-mechanical theory to analyze the multiphonon background was described in a previous work.[8] We briefly review the important features here.

The transition rate $w(\mathbf{k}_f,\mathbf{k}_i)$ for a particle making a transition from the initial incident beam of momentum $\hbar\mathbf{k}_i$ to a final state denoted by momentum $\hbar\mathbf{k}_f$ is

$$w(\mathbf{k}_f,\mathbf{k}_i)=\frac{2\pi}{\hbar}\left\langle\left\langle \sum_{\{n_f\}} |T_{fi}|^2\delta(\mathscr{E}_f-\mathscr{E}_i)\right\rangle\right\rangle , \tag{1}$$

This is the generalized Fermi golden rule, averaged over initial states of the crystal as denoted by $\langle\langle\ \rangle\rangle$, and summed over final states $\{n_f\}$ of the crystal. In Eq. (1), $\mathscr{E}_i$ and $\mathscr{E}_f$ refer to the total energy of the system of the projectile plus the crystal before and after the collision, respectively, and T_{fi} are the matrix elements of the transition operator T taken with respect to unperturbed states of the system. All measurable quantities in a scattering experiment are proportional to the transition rate. For example, the three-dimensional differential reflection coefficient, the quantity directly measured in the present experiments, is obtained by dividing $w(\mathbf{k}_f,\mathbf{k}_i)$ by the incident flux and multiplying by the appropriate density of states in final momentum space

$$\frac{d^3R}{d\Omega_f dE_f}=\frac{L^4}{(2\pi\hbar)^4}\frac{m^2|\mathbf{k}_f|}{k_{iz}}w(\mathbf{k}_f,\mathbf{k}_i) , \tag{2}$$

where L is the quantization length parallel to the surface, k_{iz} is the normal component of the incident wave vector, and m is the projectile mass.

For He atoms as incident projectiles, the dominant contribution to the multiphonon scattering comes from low-energy, long-wavelength phonons. Thus for calculating the multiphonon scattered intensity a quick scattering approximation, in which the collision time is assumed to be short compared to the relevant phonon periods, is justified.

When the quick collision approximation is combined with the generalized Fermi golden rule, after suitably averaging over the crystal modes,[20] the differential scattered intensity appears as the Fourier transform of the exponential of the time-dependent displacement correlation function:

$$\begin{aligned}\frac{d^3R}{d\Omega_f dE_f}=&\frac{m^2|\mathbf{k}_f|}{8\pi^3\hbar^5k_{iz}}\\ &\times\int_{-\infty}^{+\infty}dt\,e^{-i\omega t}\\ &\times\sum_j|\tau_{fi}|^2e^{-i\mathbf{k}\cdot\mathbf{r}_l}e^{-2W_l(\mathbf{k})}\\ &\times e^{\langle\langle\mathbf{k}\cdot\mathbf{u}_0(0)\mathbf{k}\cdot\mathbf{u}_l(t)\rangle\rangle} ,\end{aligned} \tag{3}$$

where $\mathbf{r}_l$ is the equilibrium position of the lth target center, $\mathbf{u}_l(t)$ is the displacement from equilibrium position, $\tau_{\mathbf{k}_f,\mathbf{k}_i}$ is the scattering amplitude of a surface unit cell, and $\mathbf{k}=\mathbf{k}_f-\mathbf{k}_i$. The quantity $\exp[-2W_l(\mathbf{k})]$ is the classic expression for the Debye-Waller factor, $\hbar\omega=E_f-E_i$ is the energy gained by the particle and $\langle\langle\mathbf{k}\cdot\mathbf{u}_0(0)\mathbf{k}\cdot\mathbf{u}_l(t)\rangle\rangle$ is the time-dependent displacement correlation function which can be developed in terms of the normal modes of the crystal.

This quick collision approximation is equivalent to assuming that the scattering amplitude $\tau_{\mathbf{k}_f,\mathbf{k}_i}$ is independent of the lattice displacement $\mathbf{u}_l$ of a unit cell, and the only dependence on displacement is in the phase factor. The scattering amplitude $\tau_{\mathbf{k}_f,\mathbf{k}_i}$ is, to lowest order, the off-energy-shell transition matrix element of the elastic part of the interaction potential.

The exponential of the displacement correlation function in Eq. (3) can be expanded to yield an ordered series in numbers of phonons transferred in a scattering event. The elastic and single-phonon contributions are obtained upon expanding the exponential to zero or first order in the displacement correlation function, respectively, and the multiphonon part is then contained in the remaining terms of the expansion.

Model calculations

In the semiclassical limit, we can expand the crystal displacement in a series in $\mathbf{Q}\cdot\mathbf{R}_l$, where $\mathbf{R}_l$ is the parallel component of $\mathbf{r}_l$, and $\mathbf{Q}$ is the parallel wave vector of the phonon. Then the differential reflection coefficient can be cast into the following form:[8]

$$\frac{d^3R}{d\Omega_f dE_f}=\frac{m^2|\mathbf{k}_f|}{8\pi^3\hbar^5 k_{iz}}|\tau_{fi}|^2 e^{-2W(\mathbf{k})}S(\mathbf{K},\omega)I(\mathbf{K},\omega)\ . \tag{4}$$

This is the product of a form factor $|\tau_{fi}|^2$, a Debye-Waller factor, a structure factor of $S(\mathbf{K},\omega)$, and an energy exchange factor $I(\mathbf{K},\omega)$.

When the Debye model approximation is used, these expressions take the following explicit forms:

$$S(\mathbf{K},\omega)=\sum_l e^{-i\mathbf{K}\cdot\mathbf{R}_l}\exp\left[\frac{-\omega_0 k_B T\mathbf{R}_l^2}{2\hbar v_R^2}\right], \tag{5}$$

and

$$I(\mathbf{K},\omega)=\int_{-\infty}^{+\infty}dt\, e^{-i(\omega+\omega_0)t}\exp\left[\frac{2W(k)\sin(\omega_D t)}{\omega_D t}\right], \tag{6}$$

where $\hbar\mathbf{K}$ is the parallel momentum transfer, v_R is a weighted average of phonon velocities parallel to the surface and can be taken as approximately the Rayleigh velocity for the surface modes,[21,22] ω_D is the Debye frequency, and T is the surface temperature. The quantity $\hbar\omega_0=\hbar^2k^2/2M$ is the energy shift due to the recoil motion of the crystal, with M the molecular mass of the crystal. The evaluation is made in the high-temperature limit.

Equations (4), (5), and (6) are used for the calculations to compare with the data (see below). In these calculations, for the form factor $|\tau_{fi}|^2$, we have adopted expressions obtained from the distorted-wave Born approximation, namely a Mott-Jackson matrix element for perpendicular motion and a cutoff factor for parallel motion:[23,24]

$$|\tau_{fi}|^2=e^{-K^2/Q_c^2}v_{M-J}^2(k_{fz},k_{iz})\ . \tag{7}$$

The Mott-Jackson factor v_{M-J} is the matrix element of the one-dimensional potential $v(z)=\exp\{-\beta z\}$ taken with respect to its own distorted eigenstates. The form factor (7) has a Gaussian form in K, and the Mott-Jackson factor behaves roughly as an exponential decay in the normal momentum difference $|k_{fz}|-|k_{iz}|$ when this quantity is sufficiently large.

IV. DISCUSSION OF THE RESULTS

Figure 1 shows a sample plot of the TOF data and the comparison with the preliminary calculations based on the theory. The data were taken for a crystal temperature of 155 K with a beam energy of 30 meV at specular incidence. The figure shows the combined specular and diffuse elastic peak at $\Delta E=0$ and a prominent inelastic background. However, a careful examination of the experimental data suggests a strong contribution from single phonons as well as from the coherent multiphonon part in the observed inelastic background, as might be expected for such a low surface temperature and a moderate incident energy.

A broad diffuse single-phonon contribution can arise from coherent scattering by the surface projected bulk modes or from incoherent scattering by disorder on the surface.[25] In either case, since low-frequency modes are expected to dominate, a reasonable approximation would be to calculate this single-phonon contribution with the same Debye model used for the multiphonon part. There may be some inelastic energy exchange with the hindered rotational modes of the CN^- ions in their modified K^+ cages. At the level of the present theoretical treatment, these modes are also treated within the Debye model. The resultant theory curve is pictured as a solid line in Fig. 1. The very noticeable sharp drop in intensity around 11 meV on the theory curve is the well-known discontinuity arising from the use of the Debye model.[26]

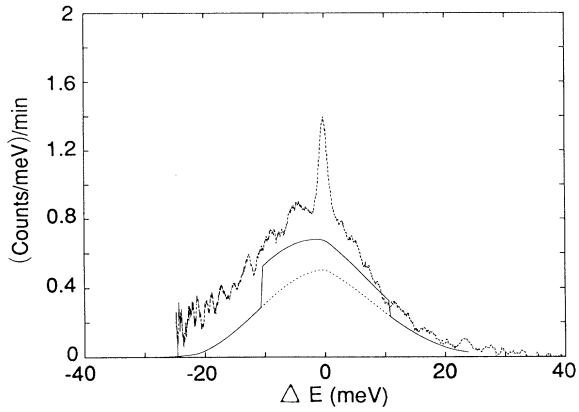

FIG. 1. Example of the comparisons made between the theory and data. The jagged line shows the experimental TOF spectrum transformed into an energy gain/loss plot for helium scattering from KCN(001) at 155 K at specular incidence with a particle energy of 30 meV. The dotted line is the calculated multiphonon background. The solid line is the theory curve after adding the single-phonon part to the multiphonon background. The assumed values of the parameters are as follows. The Debye temperature is 123 K, the molecular mass is 65.1 amu, $\beta=5.5$ Å^{-1} and $Q_c=7.5$ Å^{-1}.

This can be explained by examining the expression for the frequency distribution for the Debye model,

$$\rho(\omega)=3\omega^2/\omega_D^3 \quad \text{for } \omega \leq \omega_D \ . \tag{8}$$

At $\omega=\omega_D$ the frequency distribution abruptly drops to zero. This cutoff in the frequency spectrum in turn causes the unphysical behavior of the single-phonon intensity calculated using the Debye model, as illustrated in the figure. To overcome this problem, we have assumed a correcting factor to the Debye spectrum which eliminates the abrupt fall in the frequency distribution at $\omega=\omega_D$. The modified frequency distribution function is

$$\rho(\omega)=3\omega^2/\omega_D^3 \quad \text{for } |\omega| \leq \omega_1 \tag{9}$$

and

$$\rho(\omega)=\frac{3\omega^2}{\omega_D^3} e^{-(|\omega|-\omega_1)^2 A^2} \quad \text{for } |\omega| > \omega_1 \ , \tag{10}$$

where ω_1 is an intermediate value in the frequency spectrum slightly smaller than ω_D and A is a constant. For our best match we have used $A=3.18$ (s/rad) and $\omega_1=0.7\omega_D$, and these leave the integral of $\rho(\omega)$ still normalized to unity. Using the modified spectrum the theory curve assumes a much better appearance, as depicted in Fig. 2, which is for the same experimental configuration as in Fig. 1. The discontinuities in intensity at the Debye energies of ± 11 meV are now replaced by smooth curves as a result of the modified Debye spectrum that the calculations are based on. The shoulders seen in the calculated result at an energy exchange of around ± 11 meV are clearly evident in the experimental data, which is a strong indication of the correct value of the Debye frequency.

The actual determination of the Debye temperature is obtained from a Debye-Waller plot of the elastic intensity at the specular position. The logarithmic plot of the elastic data (with the diffuse inelastic background subtracted) versus surface temperature is shown in Fig. 3, and is nearly linear. This is compared to the theoretical form

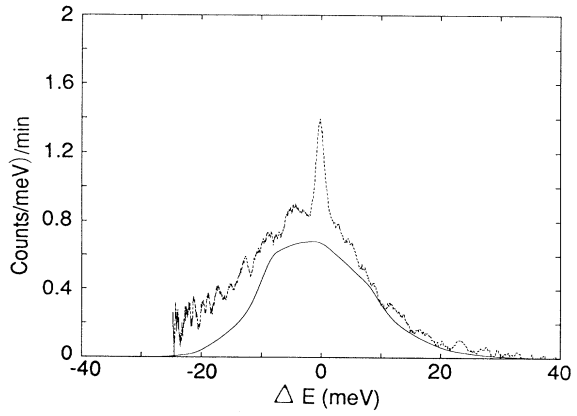

FIG. 2. Example of the comparisons made between the theory and data using the modified Debye spectrum. The experimental data and the theoretical parameters are the same as in Fig. 1.

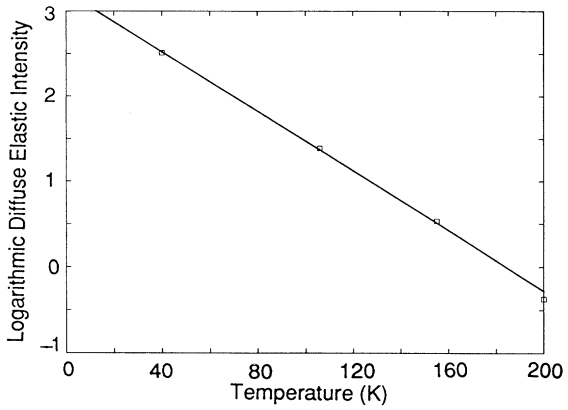

FIG. 3. Natural logarithm of the elastic peak height vs temperature for helium scattering from KCN (001).

$I(T)=I(0)e^{-2W}$, with $2W$ calculated within the Debye model as

$$2W(\mathbf{k})=\frac{3|\mathbf{k}|^2 k_B T}{M\omega_D^2} \ . \tag{11}$$

For a molecular mass of 65.1 amu (K+C+N), a linear fit of Eq. (11) to the experimental data of Fig. 3 yields 123 K for the Debye temperature (or 11.2 meV for the Debye energy).

Figure 4 presents a summary of the comparisons carried out at the specular position for crystal temperatures range from 40 to 334 K. The predicted multiphonon background and the calculated total inelastic intensity (the sum of multiphonon and single-phonon parts) are plotted along with the experimental data taken for a beam energy of 30 meV. For all calculations the Debye temperature is 123 K, the molecular mass is 65.1 amu, $\beta=5.5$ Å^{-1}, and $Q_c=7.5$ Å^{-1}. In each panel the solid line is the experimental result, the dashed line is the theoretical calculation including both single and multiphonon contributions, and the dotted line gives the calculated multiphonon contribution alone.

One can clearly see that, as the temperature increases, the elastic peak decreases according to the Debye-Waller behavior exhibited in Fig. 3, while the inelastic background broadens in width. The maximum intensity of the background, however, remains relatively unchanged for the lower-temperature runs, but decreases somewhat at higher temperatures. At the highest temperatures the single-phonon contribution becomes negligible due to the attenuation by the Debye-Waller factor, and nearly all the inelastic scattering is multiphonon.

Calculations of the maximum multiphonon peak height and the full width at half maximum (FWHM) as a function of surface temperature agree quite well with the experimental data. The behavior of the maximum multiphonon intensity and FWHM as a function of temperature can be qualitatively explained on the basis of unitarity arguments. The increasing width is due to the larger number of scattering channels available with increasing temperature. However, above the temperature at which the elastic and single-phonon quantum contributions

have disappeared, the maximum value of the inelastic intensity decreases in order to conserve the total number of scattered particles. This agreement between calculation and experiment is an indication that the multiphonon scattering does not depend strongly on the nature of the frequency distribution.

Figure 5 shows the comparisons with the data taken at off-specular angles. The crystal temperature here was 180 K, the incident beam energy 28.1 meV, and the angles of incidence range from $\theta_i = 53°$ to the specular angle $\theta_i = 45°$. For the theoretical calculations all parameters are taken to be the same as in Fig. 4. At this relatively low surface temperature the single-phonon contribution is still substantial. As in Fig. 4, the theory somewhat underestimates the total elastic background near specular incidence, but agrees well at larger angles away from specular. This near-specular scattering may be significantly enhanced compared to the present model due to the long-range Van der Waals forces of defects.

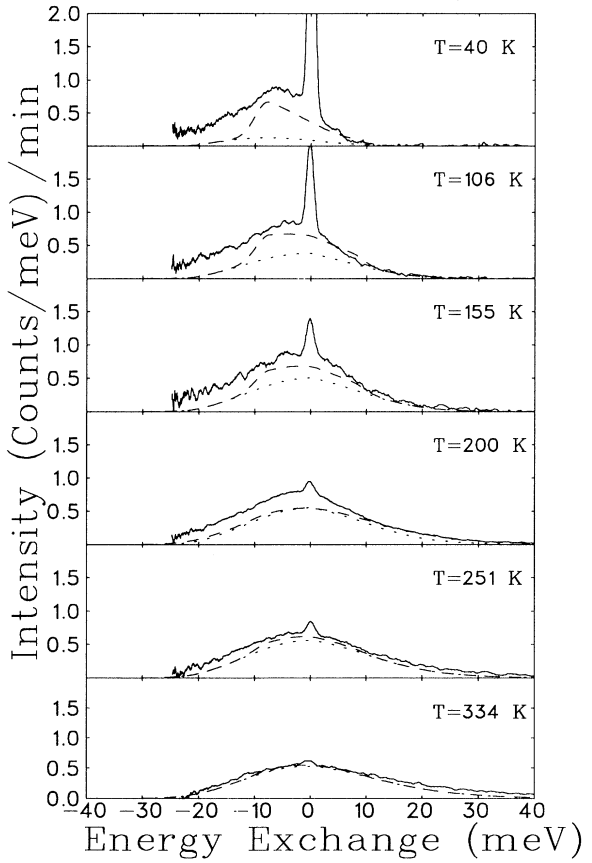

FIG. 4. Intensity vs energy exchange curves for He scattering from KCN at 45° incidence for different substrate temperatures. The dotted lines indicate the calculated multiphonon backgrounds. The dashed lines are the theory curves (single-phonon plus multiphonon contributions) to match with the data curves represented by solid lines. The incident energy and other parameters are the same as in Fig. 1.

V. CONCLUSIONS

Here we have presented an experimental and theoretical study of the inelastic background observed in He-atom scattering from the cleaved (001) surface of KCN. The He beam has an energy of approximately 30 meV, and observations of the energy-resolved scattered distribution are made at several incident polar angles and over a range of temperatures from 40 to 350 K. At high temperatures, above 200 K, the scattered intensity consists entirely of a broad multiphonon inelastic feature with a single maximum, with no sharp elastic or single-phonon peaks. At lower temperatures there is evidence of a strong single-phonon contribution in the inelastic background, but there are no sharp single-phonon peaks due to localized surface modes and the elastic features consist of a diffuse elastic peak seen at all angles which merges into a much stronger elastic peak at the approximate specular position. No higher-order diffraction peaks are observed in angular distributions of scattered intensity versus incident angle.

Neutron-scattering experiments from bulk KCN have indicated a rather large diffuse elastic and inelastic background indicative of a significant amount of disorder.[13,15] The absence of diffraction peaks and peaks in the TOF

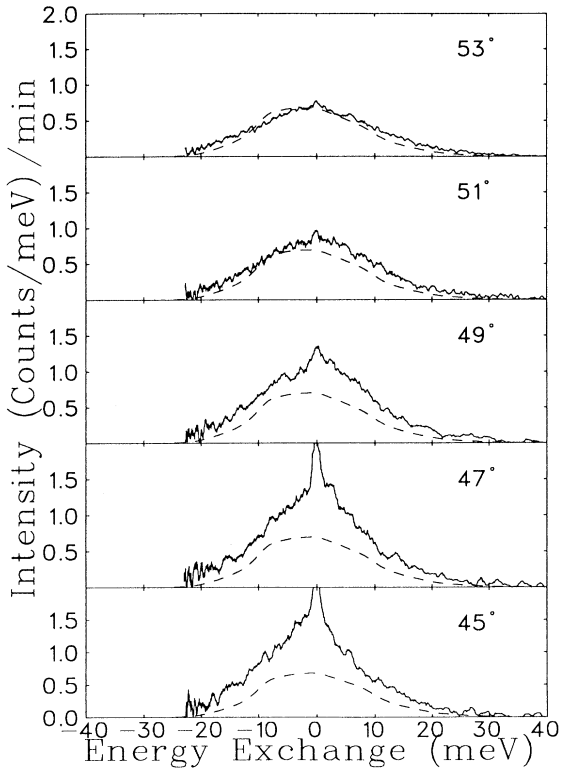

FIG. 5. Intensity vs energy exchange curves for He scattering from KCN at 180 K for different angles of incidence and the incident energy of 28.1 meV. The dashed lines are the theory curves (single-phonon plus multiphonon contributions) to match with the data curves represented by solid lines. The other parameters are the same as in Fig. 1.

spectra due to Rayleigh or other localized surface modes in these observations is indicative that this surface is more disordered than the bulk. The disorder is probably due in part to the orientational disorder of the CN^- ions, whose cages of K^+ ions are opened at the cleaved (001) surface. Because of the different orientational order of the much larger CN^- ions from cell to cell, the translational symmetry of the crystal is destroyed.[12] However, since any long-range order of the unit cells themselves can still give to diffraction peaks, it is not clear that orientational disorder alone can account for their absence here. Regardless, the complete absence of diffraction peaks indicates long-range lattice disorder on the surface. It is clear that more information is needed to understand the nature of this disorder.

The observed temperature range encompasses the two known phase transitions in bulk KCN at $T=168$ and 83 K. Unlike in the bulk, no unusual surface behavior in either the elastic or inelastic scattered intensity is observed in the neighborhood of either of these two transition temperatures.

The theoretical model used to interpret the data is based on a quick collision approximation, which should be adequate for the exchange of large numbers of small frequency phonons, and uses a Debye model for the phonon frequency distribution.[8,9] The influence of the interaction potential between the particle and the surface enters through a form factor which is essentially the squared modulus of the transition matrix for scattering from a single unit cell. For this form factor we have chosen a product of a Mott-Jackson matrix element for perpendicular motion and a Gaussian cutoff factor for parallel motion, a choice motivated by distorted-wave perturbation theory, and one which has been shown useful for both single- and multiple-phonon scattering.[2–6,9,24]

The single-phonon contribution is also calculated using the Debye model. For a clean ordered surface this would normally be considered a poor approximation, because the sharp features of the single-phonon contribution can be reproduced only by using an accurate and realistic phonon spectral density. However, for this surface the single-phonon contribution to the total scattered intensity is smooth and diffuse with no sharp features. This would imply that the single-phonon intensity is dominated by scattering from bulk modes and from diffuse scattering from surface defects, and both these contributions can be reasonably modeled by a Debye frequency distribution. At temperatures lower than 100 K the single-phonon part of the intensity is rather prominent, and its features are well matched by the Debye model calculation. In fact, the Debye model predicts a sharp cutoff shoulder in the energy-resolved intensity at energy gains and losses corresponding to the Debye frequency. The good match between the positions of this shoulder in the calculated and measured intensities at low temperatures serves as a secondary method for determining the surface Debye temperature, the primary method for determination of the Debye temperature being a fit to the Debye-Waller factor for the decrease of the elastic specular peak with temperature. The Debye-Waller fit gives a Debye temperature of 123 K which is consistent with the positions of the observed shoulders in both the energy-gain and -loss sides of the experimental data at the lowest temperatures.

The agreement between theory and experimental data is good at all temperatures and incident angles, with the best agreement occurring at high temperatures where the intensity is dominated by the multiphonon contribution and looks very much like a smooth classical scattering distribution with no sharp quantum features. The good match at high temperatures enables a determination of the β and Q_c parameters of the form factor. The best choices for all the data measured are $\beta=5.5$ Å^{-1} and $Q_c=7.5$ Å^{-1}. Both these values are large compared to the typical values of $\beta\approx 2-3$ Å^{-1} and $Q_c\approx 1-2$ Å^{-1}, which have been obtained from examinations of the momentum dependence of the single-phonon peaks measured on close-packed metal surfaces.[7] Larger values of the potential range parameter β are expected for the more rigid surface of an insulator such as KCN. The larger value of Q_c is indicative of a rougher surface which tends to scatter particles to larger parallel momentum values, as compared to a close-packed metal. However, the very large values of these two parameters implies a form factor which has very little dependence on either normal or parallel momentum transfer; i.e., it implies nearly uniform scattering in momentum space with a cutoff at values of parallel and perpendicular momenta only for particle wave vectors larger than β and Q_c, respectively. This result is again consistent with scattering from a rather rough surface in which the unit cells can deflect the incident particles to very large angles away from the specular direction.

The good agreement between theory and experiment implies that with this rather straightforward and readily calculable theory we have a tool which will be useful for determination of the multiphonon contribution to the entire diffuse inelastic background. This information is particularly useful for purposes of subtraction from the data in order to determine the true experimental values for the elastic and single quantum features.[4,6,7] The agreement also substantiates the fundamental assumption that the multiphonon contribution should not depend strongly on the phonon spectral density. Because of this insensitivity to the phonon distribution, the inelastic background at high temperatures can be used to determine the range and cutoff parameters of the interaction potential for inelastic scattering.

ACKNOWLEDGMENTS

This research was supported by DOE Grant No. DE-FG05-85ER45208, NSF Grant No. DMR 9419427, and NATO Grant No. 891059. J.R.M. and J.G.S. thank Professor J. P. Toennies and the Max Planck Institut für Strömungsforschung for their hospitality in providing a stimulating environment during the completion of part of this work.

[1]J. P. Toennies, in *Surface Physics,* edited by W. Kress (Springer-Verlag, Berlin, 1991), Chap. 5.
[2]J. G. Skofronick, G. G. Bishop, W. P. Brug, G. Chern, J. Duan, and S. A. Safron, Superlatt. Microstruct. **7**, 239 (1990).
[3]S. A. Safron, W. P. Brug, G. Chern, J. Duan, and J. G. Skofronick, J. Vac. Sci. Technol. A **8**, 2627 (1990).
[4]G. G. Bishop, W. P. Brug, G. Chern, J. Duan, S. A. Safron, and J. G. Skofronick, Phys. Rev. B **47**, 3966 (1993).
[5]J. R. Manson and J. G. Skofronick, Phys. Rev. B **47**, 12 890 (1993).
[6]G. G. Bishop, E. S. Gillman, J. J. Hernández, J. Baker, J. G. Skofronick, and S. A. Safron, J. Vac. Sci. Technol. A **12**, 2124 (1994).
[7]F. Hofmann, J. P. Toennies, and J. R. Manson, J. Chem. Phys. **101**, 10 155 (1994).
[8]J. R. Manson, Phys. Rev. B **43**, 6924 (1991).
[9]J. R. Manson, Comput. Phys. Commun. **80**, 145 (1994).
[10]J. M. Rowe, J. J. Rush, and E. Prince, J. Chem. Phys. **66**, 5147 (1977).
[11]K. H. Michel and J. Naudts, J. Chem. Phys. **67**, 547 (1977).
[12]W. Dultz, Solid State Commun. **15**, 595 (1974).
[13]J. M. Rowe, J. J. Rush, N. Vagelatos, D. L. Pierce, D. G. Hinks, and S. Susman, J. Chem. Phys. **62**, 4551 (1975).
[14]J. M. Rowe, J. J. Rush, N. J. Chesser, K. H. Michel, and J. Naudts, Phys. Rev. Lett. **40**, 455 (1978).
[15]D. Strauch, U. Schröder, and W. Bauernfeind, Solid State Commun. **30**, 559 (1979).
[16]G. Chern, J. G. Skofronick, W. P. Brug, and S. A. Safron, Phys. Rev. B **39**, 12 828 (1989).
[17]D. M. Smilgies and J. P. Toennies, Rev. Sci. Instrum. **59**, 2185 (1988).
[18]J. P. Toennies, in *Surface Phonons,* edited by W. Keiss and F. Wide Wette, Springer Series in Surface Sciences Vol. 21 (Springer, Heidelberg, 1991), p. 111.
[19]Utah Crystal Growth Laboratory, University of Utah, Physics Department, Salt Lake City, UT 84112.
[20]A. A. Maradudin, E. W. Montroll, and G. H. Weiss, in *Theory of Lattice Dynamics in the Harmonic Approximation, Solid State Physics,* edited by F. Seitz and D. Turnbull (Academic, New York, 1963), Suppl. 3.
[21]R. Brako and D. M. Newns, Phys. Rev. Lett. **48**, 1859 (1982).
[22]R. Brako and D. M. Newns, Surf. Sci. **123**, 439 (1982).
[23]F. O. Goodman and H. Y. Wachman, *Dynamics of Gas-Surface Scattering* (Academic, New York, 1976).
[24]V. Celli, G. Benedek, U. Harten, J. P. Toennies, R. B. Doak, and V. Bortolani, Surf. Sci. **143**, L376 (1984).
[25]J. Manson and V. Celli, Phys. Rev. B **39**, 3605 (1989).
[26]A. Sjölander, Ark. Fys. **14**, 315 (1959).